



Dynamic modeling of lithium-ion battery degradation using data-driven and physics-informed method

Daniel Santoso¹, Muhamad Dzaky Ashidqi^{2,3*}

¹Department of Electronic and Computer Engineering, Universitas Kristen Satya Wacana, Indonesia

²Department of Electrical Engineering and Information Technology, Universitas Gadjah Mada, Indonesia

³Department of Electrical Engineering, Universitas Sains Indonesia, Indonesia

Abstract

Accurate real-time prediction of lithium-ion battery (LIB) capacity degradation is essential for embedded battery-management systems. Equivalent circuit models (ECMs) run quickly but lose accuracy over time, whereas purely data-driven networks achieve high precision at a high computational cost. This study introduces a physics-informed neural network (PINN) that embeds the differential equations of a first-order Thevenin ECM directly into the loss function. Using only terminal voltage and current as inputs, the network simultaneously estimates internal resistance, polarization resistance, polarization capacitance, open-circuit voltage, and capacity loss. The model was trained and evaluated over 300 charge-discharge cycles of an 18650 lithium-ferrous phosphate (LFP) cell. The resulting capacity degradation estimation achieved a root mean squared error (RMSE) of 0.012 and a mean absolute percentage error (MAPE) of 0.974 %, surpassing a neural ordinary differential equation baseline with RMSE of 0.215. The trained network contains 261 parameters, requires 0.6 ms per sample for inference, and consumes 49 MB of memory. This computation cost is far lower than that of a long short-term memory (LSTM) benchmark with comparable accuracy. In addition, the proposed model maintains its accuracy under limited dataset conditions. With a fourfold smaller training set, the PINN maintained an RMSE of 0.023, whereas the LSTM error increased to 0.72. The results demonstrate that lightweight neural networks guided by physics-based constraints can provide reliable, real-time health estimation on resource-limited hardware.

Keywords:

Capacity degradation;
Equivalent Circuit Model;
Lithium-Ion Battery;
Neural Network;

Article History:

Received: April 28, 2025

Revised: July 19, 2025

Accepted: August 1, 2025

Published: January 7, 2026

Corresponding Author:

Muhamad Dzaky Ashidqi
Department of Electrical
Engineering,
Universitas Sains Indonesia
Email:

muhamad.dzaky@lecturer.sains.ac.id

This is an open-access article under the CC BY-SA license.



INTRODUCTION

The extensive use of lithium-ion batteries in energy storage systems (BESS) has driven advancements in accurate battery degradation modeling [1]. Battery degradation impacts, system performance, safety, and economic viability [2]. Understanding and predicting battery degradation processes under various operating conditions remains a significant challenge. This challenge is compounded by the highly nonlinear nature of battery degradation mechanisms, including chemical, thermal, and mechanical effects [3]. Therefore, developing a robust and accurate

battery degradation model remains a significant gap [4].

Physics-based models have been extensively developed to understand and simulate the mechanisms underlying battery degradation. These models are generally divided into two main categories: electrochemical models [5][6] and electrical equivalent circuit models (ECMs) [7][8]. Electrochemical models are known for their high accuracy in capturing the internal physicochemical processes of batteries. However, they often require intensive computation and detailed knowledge of battery chemistry, which limits their

application in real-time systems. In contrast, ECMs are gaining popularity for short-term prediction and state estimation tasks due to their simplicity and computational efficiency [9]. These models predict battery behavior using electrical components, making them practical for embedded systems and battery management applications.

Several types of ECMs have been developed to model battery behavior with varying degrees of complexity. Among the most commonly used are the simple linear model [10], the first-order Thevenin model consisting of one parallel resistor-capacitor (R-C) [11], the second-order R-C model [7], and the Partnership for a New Generation of Vehicles (PNGV) model [12]. These models are preferred due to their computational efficiency, fewer parameters, and suitability for real-time implementation [9]. Despite its advantages, ECM has limitations in accurately representing the complex, nonlinear degradation mechanisms that occur over the battery's lifetime [13]. Therefore, although ECM is effective for operational monitoring and control, it may not have the precision required for long-term degradation prediction and analysis.

Recent advances in battery degradation modeling increasingly rely on data-driven approaches, particularly machine learning (ML) techniques. These methods have gained widespread attention due to their ability to capture nonlinear and complex battery degradation patterns without the need for detailed physical or chemical models [14]. Unlike traditional physics-based models, ML techniques can learn directly from historical battery data to identify trends and predict degradation trajectories. Several ML algorithms have been explored by researchers, such as random forest (RF) [15], XGBoost [16], convolutional neural networks (CNN) [17], recurrent neural networks (RNN) [18], and long short-term memory (LSTM) networks [19], each offering different strengths in handling time-series and high-dimensional data.

RF and XGBoost are ensemble learning methods based on decision trees, known for their robustness and interpretability, especially when dealing with structured tabular data [15][16]. CNNs have shown promising results in extracting local patterns from battery time-series data and sensor signals due to their strong feature-extraction capabilities [17]. RNNs are designed to model sequential data and can capture temporal dependencies, though they may suffer from vanishing gradients [18]. To address this, LSTM, an advanced variant of RNN, combines memory cells and gating mechanisms, making it more suitable for long-term sequence modeling and

degradation trend estimation [19]. Another ML technique, such as Gaussian process regression (GPR), uses Bayesian and statistical learning theory. Therefore, it can quantify prediction uncertainties, which is important for assessing the reliability of battery health estimation [20].

These ML models have demonstrated strong performance in predicting key battery parameters, including capacity fade, internal resistance, and state of health across diverse operating conditions [21]. Their ability to generalize from large datasets makes them suitable for condition monitoring and predictive maintenance in battery systems. However, despite their high predictive accuracy, purely data-driven methods face several challenges [22]. One of the main limitations is the lack of interpretability, which can make it challenging to understand the physical mechanisms underlying degradation. Furthermore, these models often require large, high-quality training datasets to ensure robustness and avoid overfitting, which may not always be available in practical applications [23]. Consequently, while ML techniques offer high performance compared to traditional modeling approaches, careful consideration of data requirements and transparency is critical in battery applications.

Techniques such as grey relational analysis (GRA) and principal component analysis (PCA) have been used to remove redundant data and reduce dimensionality [24][25]. These methods improve model efficiency by minimizing computational overhead and focusing on the most relevant features. However, preprocessing steps can add complexity to the modeling process and may require significant domain expertise to implement effectively. These limitations highlight the need for hybrid solutions that balance the strengths of physics-based and data-driven approaches [26].

Several researchers have proposed hybrid approaches that integrate physics-based insights with data-driven methods. Ashidqi et al. proposed a hybrid method using a perceptron and the Thevenin equivalent circuit model [27]. Similarly, Fan et al. introduced a physics-informed integrated modeling method that combines electrochemical modeling with machine learning to improve degradation predictions [28]. These methods demonstrated enhanced accuracy and are computationally lightweight. However, the models developed were unable to interpret the dynamics of battery degradation.

To implement hybrid approaches for dynamic models of battery degradation, physics-based models using ECM can be utilized [27]. The

Table 1. Summary of battery degradation dynamic modeling approaches

| Model Category | Modeling Approach | Key Strengths | Limitations |
|-------------------------------------|---|---|---|
| Electrochemical Model | Arrhenius Electrochemical Models [5][6] | High accuracy; captures fundamental physicochemical processes | High computational cost; complex parameterization; not suitable for real-time use |
| Electrical Equivalent Circuit Model | Thevenin (1 st -order) [11] 2 nd -order R-C model [7] PNGV model [12] | Simple structure; suitable for real-time applications; low computational load More accurate than 1 st -order; still computationally efficient Suitable for real-time; improved accuracy | Limited accuracy in nonlinear degradation modeling Still limited in modeling long-term nonlinear behavior Reduced accuracy in highly dynamic conditions |
| Machine Learning | RF [15], XGBoost [16] CNN [17] RNN [18] LSTM [19] | Robust; interpretable; works well with tabular data Excellent feature extraction from structured signals Handles sequential data; models temporal behavior Captures long-term dependencies; effective in trend forecasting | Requires labeled data; not suitable for sequence modeling Lacks temporal memory; limited in capturing long-term dependencies Suffers from vanishing gradients; lower stability Requires more training data and parameters; slower to train |
| Hybrid Method | NODE [29] | Captures voltage dynamics; interpretable | High data requirement; limited adaptability to new conditions |

dynamic equation from the ECM can then be combined with the ML technique to create a grey-box model. Brucker et al. developed a grey-box model using a neural ordinary differential equation (NODE) to capture the slow voltage dynamics of lithium-ion batteries [29]. While effective in simplifying the representation of slow dynamics, this approach requires extensive training data and is less adaptable to varying operating conditions. Martinez et al. present a dynamic model that combines machine learning with Thevenin equivalent circuits for battery health diagnosis and prognosis [30]. While these models achieve better control over health awareness, their reliance on extensive feature sets and complex parameter identification processes poses challenges for real-time applications and scalability.

Despite the progress made by these studies, several challenges remain unresolved. Existing models often require high-dimensional feature sets, complex parameter tuning, or computationally intensive training processes. Furthermore, while integrating data-driven methods with ECM is promising, it still faces challenges in ensuring simplicity and adaptability without sacrificing accuracy [31].

In this study, a novel hybrid approach is proposed for dynamic modeling of battery degradation by integrating artificial neural networks (ANN) with the Thevenin equivalent circuit model. Unlike previous studies, the proposed method relies on only two input features -- terminal voltage and current -- thereby simplifying the modeling process, reducing the amount of data required, and preserving high

prediction accuracy. This method addresses key limitations of existing approaches by lowering computational complexity and minimizing dependence on extensive feature sets. To train the model, a pulse test is conducted to extract key parameters such as open-circuit voltage, polarization resistance, polarization capacitance, and internal resistance, which are used in a physics-informed neural network (PINN) framework.

The performance of the proposed method is evaluated through comparative analysis against established techniques, including NODE and LSTM networks. Model performance is assessed by using root mean square error (RMSE) and mean absolute percentage error (MAPE) to measure prediction accuracy. In addition, computational efficiency is evaluated by comparing inference time, memory usage, and the number of parameters. This comprehensive analysis demonstrates the effectiveness of the proposed method for accurately, interpretably, and efficiently modeling battery degradation across various operating conditions.

METHOD

In this study, the dynamic battery degradation model will be obtained by incorporating domain knowledge derived from a first-order Thevenin model into the loss function of an ANN. This method aims to bridge the gap between data-driven and physics-based approaches. The steps taken in this study are described in the subsections below.

Physics-based model

A physics-based model is required to derive a dynamical equation for the battery that can be used to estimate its capacity degradation. In this study, the first-order Thevenin equivalent circuit model is utilized due to its simplicity and sufficient accuracy [8]. The first-order Thevenin equivalent circuit model is a simplified representation of a battery's electrical behavior, consisting of an open-circuit voltage (OCV) in series with a resistor (R) and a parallel resistor-capacitor (R-C) network, as shown in Figure 1.

The voltage across the battery terminals, V_t , is expressed as (1):

$$V_t(t) = V_{oc}(t) - I_b(t) \cdot R_i(t) - V_{RC}(t) \quad (1)$$

Where V_{oc} is the open circuit voltage, I_b is the current across the battery, R_i is the internal resistance, and V_{RC} is the voltage in the R-C branch. V_{RC} can be written as (2):

$$V_{RC} = I_b R_i (1 - e^{-t \left(\frac{R_p}{C_p} \right)}) \quad (2)$$

Where R_p and C_p are the resistance and capacitance in the parallel R-C branch. The parameters R_i , R_p , C_p , and V_{oc} evolve with battery aging and are used to estimate battery degradation. The dynamics of R_p and C_p then can be expressed as (3):

$$\frac{dV_{RC}(t)}{dt} = \frac{I_b(t)}{C_p(t)} - \frac{V_{RC}(t)}{R_p(t) \cdot C_p(t)} \quad (3)$$

The capacity degradation of the battery can be calculated by measuring the change in internal resistance (R_i) and polarization capacitance (C_p). Capacity degradation will increase as internal resistance rises and polarization capacitance decreases. Thus, the relation between R_p , C_p , and capacity degradation can be mathematically written as (4):

$$\Delta Q(t) = \frac{C_p(0)}{C_p(t)} \cdot \frac{R_i(t)}{R_i(0)} \quad (4)$$

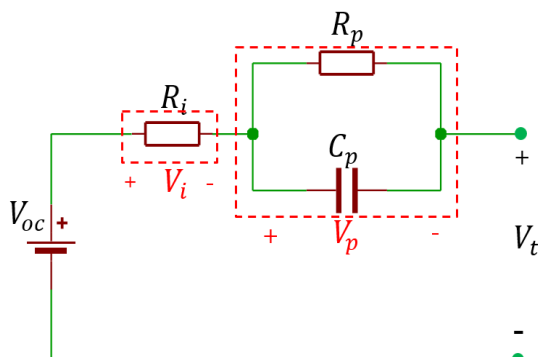


Figure 1. The first-order Thevenin equivalent circuit model

$\Delta Q(t)$ represents capacity degradation, which can be measured in percentage. Equation (4) shows that the actual capacity degradation can be measured by determining the initial polarization capacitance $C_p(0)$, the initial internal resistance $R_i(0)$, the actual polarization capacitance $C_p(t)$, and the actual internal resistance $R_i(t)$.

Dataset Preparation

The parameters required for the dataset are determined from the battery dynamic equations. In the previous subsection, the dynamic model was obtained using the first-order Thevenin equivalent circuit model as expressed in (2) and (3). From (2) and (3), it can be inferred that the parameters needed to complete the dynamic model are V_t , I_b , R_i , R_p , C_p , and V_{oc} . To collect the data, an experiment was conducted using a battery tester unit. An 18650 lithium-iron phosphate (LFP) battery was tested through a 300-cycle charging-discharging test. The charging and discharging process was conducted in a temperature-controlled chamber. The chamber temperature is maintained at 25 °C to minimize the effect of temperature changes on battery degradation.

Experimental data collected from the battery tester unit include five parameters: terminal voltage (V_t), charging-discharging current (I_b), temperature, and maximum capacity per cycle, which can indicate capacity degradation. The battery is charged and discharged using a hybrid constant-current-constant-voltage (CC-CV) charger to ensure it reaches its maximum capacity. However, the other four parameters (R_i , R_p , C_p , and V_{oc}) cannot be obtained from the experiment. Thus, additional calculations are needed to determine the initial parameter values R_i , R_p , C_p , and V_{oc} .

The pulse-discharge test and transient-response analysis method were applied to determine the initial parameter values analytically. First, a pulse discharge was applied to measure R_i . In this test, a step current (I_s) is applied to the battery, triggering a voltage drop (ΔV). The voltage drop was measured immediately after a step current was applied. Then, the internal resistance can be calculated analytically using the (5):

$$R_i = \frac{\Delta V}{I_s} \quad (5)$$

Once the internal resistance (R_i) has been determined, the open-circuit voltage (V_{oc}) can be calculated using (1) by substituting the R_i value (R_i) from (5) and I_s as I_B to determine the initial value of V_{oc} , V_{RC} , or the voltage across the R-C branch, it was assumed to be 0.

To find the initial value of R_p , another test was run. A tiny, steady current was used to deplete the battery, and the voltage reduction over time was recorded. Afterward, the steady-state voltage decay was fitted to an exponential function as shown (6):

$$V_t = V_{oc} - IR_p(1 - e^{-\frac{t}{\tau}}) \quad (6)$$

The starting value of R_p can be found by solving (6) using the steady-state value and V_{oc} value from the previous step. Following this step, the value of C_p can be determined using the time constant of the transient response that is given by (7):

$$\tau = R_p \cdot C_p \quad (7)$$

From the voltage response to the current step, the settling time τ was measured as the time required for the voltage to reach approximately 63% of its final value, which is typical for a first-order system response of an R-C circuit [32][33].

Once the initial values of all parameters have been obtained, the time-series dataset can be created using a differential equation approximation based on the Euler method, as in (1) and (3). The discrete time-series model to generate the dataset is provided by:

$$V_{RC}(t + \Delta t) = V_{RC}(t) + \left(\frac{I_b(t)}{C_p} - \frac{V_{RC}(t)}{R_p C_p} \right) \Delta t \quad (8)$$

$$V_t(t + \Delta t) = V_{oc}(t) - I_b(t)R_i - V_{RC}(t) \quad (9)$$

Δt is the sampling interval. In this research, the sampling interval is within one second. $V_{RC}(t)$ and $V_{oc}(t)$ were updated iteratively based on the battery current (I_b). Parameters calculated at each time step using the discretized equations were recorded and compiled into a dataset for training the neural network model in the next step.

ANN Model

A neural network was used to estimate the dynamics of the parameters R_i , R_p , C_p , V_{oc} , and ΔQ over time, using terminal voltage (V_t) and battery current (I_b) as inputs. Neural Networks (NNs) are employed in this study due to their strong capability to model complex, nonlinear relationships and to learn underlying patterns directly from historical data without requiring explicit mathematical formulations [34]. To create the prediction model, the dataset collected in the previous step will be used for neural network training. As there are two input and five output parameters, the ANN model was constructed with the structure shown in Figure 2. x_1 and x_2 represent the input features V_t and I_b , respectively.

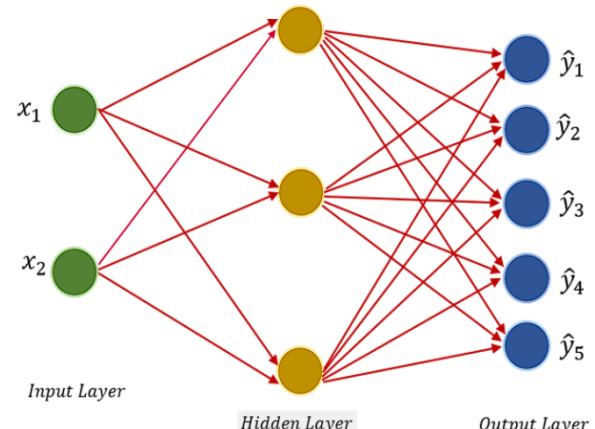


Figure 2. ANN structure for battery degradation model

In contrast, \hat{y}_1 , \hat{y}_2 , \hat{y}_3 , \hat{y}_4 , and \hat{y}_5 represent five output features: R_i , R_p , C_p , V_{oc} , and ΔQ .

The ANN model is trained using the physics-based loss function, since the study's approach is a physics-based neural network. Thus, the ANN dynamically learns parameters while satisfying the physics-based constraints imposed by the governing equations. This is achieved during training using a combined loss function that includes data-based output loss, physics-based R-C constraints, and a battery degradation (ΔQ) constraint. These loss functions are given by:

$$\mathcal{L}_{out} = \frac{1}{N} \sum_{i=1}^N |V_t(t)_{true} - V_t(t)_{pred}|^2 \quad (10)$$

$$\mathcal{L}_{RC} = \frac{1}{N} \sum_{i=1}^N \left| \frac{dV_{RC}}{dt} + \frac{1}{R_p C_p} V_{RC} - \frac{0.01}{C_p} \right|^2 \quad (11)$$

$$\mathcal{L}_{\Delta Q} = \frac{1}{N} \sum_{i=1}^N \left| \Delta Q - \frac{C_p}{3600} \cdot \frac{0.01}{R_i} \right|^2 \quad (12)$$

Equations (10), (11), and (12) provide data-driven output loss, R-C physics-based constraint, and battery degradation loss, respectively. The number of data used in the training phase is denoted by N . The overall loss then can be computed as:

$$\mathcal{L}_{total} = \mathcal{L}_{out} + \mathcal{L}_{\Delta Q} + \mathcal{L}_{RC} \quad (13)$$

During training, the NN learns how R_i , R_p , C_p , V_{oc} , and ΔQ evolve and predicts battery degradation as a function of these parameters. This method ensures real-time prediction with robust and accurate results.

RESULTS AND DISCUSSION

This section presents the findings from the data preparation and model simulation for the model proposed in this study. The data preparation results include parameter initialization and dataset construction. The acquired dataset is used to build a battery degradation model using the proposed physics-based NN method. Details of the results and their analysis are explained in the subsections below.

Data Preparation

The data generated during the experimental process include key parameters such as terminal voltage (V_t), battery current (I_b), and capacity degradation (ΔQ). The proposed model requires additional parameters, including R_i , R_p , C_p , and V_{oc} . Using (5), (6), and (7), the initial values of these parameters are obtained as shown in [Table 2](#). The initial parameter values were used to generate a time-series dataset for 300 cycles using the Euler method based on (8) and (9).

Model Simulation

The dataset obtained in the previous step was trained to build a physics-based NN model. The proposed model was successfully constructed and can be used to estimate the dynamics of the parameters R_i , R_p , C_p , and V_{oc} over cycles, providing accurate predictions of battery performance degradation in each cycle. The comparison between the estimated and actual battery degradation is shown in [Figure 3](#). This plot compares the actual battery capacity degradation and the predictions obtained from the proposed PINN model over 50 charge-discharge cycles.

Table 2. Parameters initial value

| Metrics | Proposed PINN |
|----------|---------------|
| R_i | 9.24 mΩ |
| V_{oc} | 3.54 V |
| C_p | 3.49 kF |
| R_p | 5.17 mΩ |

The actual data shows a nearly linear degradation trend with local fluctuations caused by minor operational or measurement variations. The PINN model predictions closely track this degradation curve, effectively capturing both the general trend and subtler variations across the cycle range.

The accurate alignment of the PINN prediction with the measured data indicates that the model successfully incorporates domain knowledge through the embedded physical constraints. This physics-informed structure enables the model to distinguish true degradation. Dynamics from high-frequency noise, enhancing both its predictive performance and interpretability. It is noteworthy that the PINN model remains consistent even in areas where the actual capacity shows abrupt drops (e.g., around cycles 10, 30, and 42), suggesting robust generalization. The close correspondence between the prediction and ground truth supports the hypothesis that incorporating physical laws into the learning framework improves the modeling of battery capacity fade.

To assess model performance, the degradation estimates from the proposed model are compared with those from previous methods. The methods developed in previous research for comparison are LSTM [19] and NODE [29].

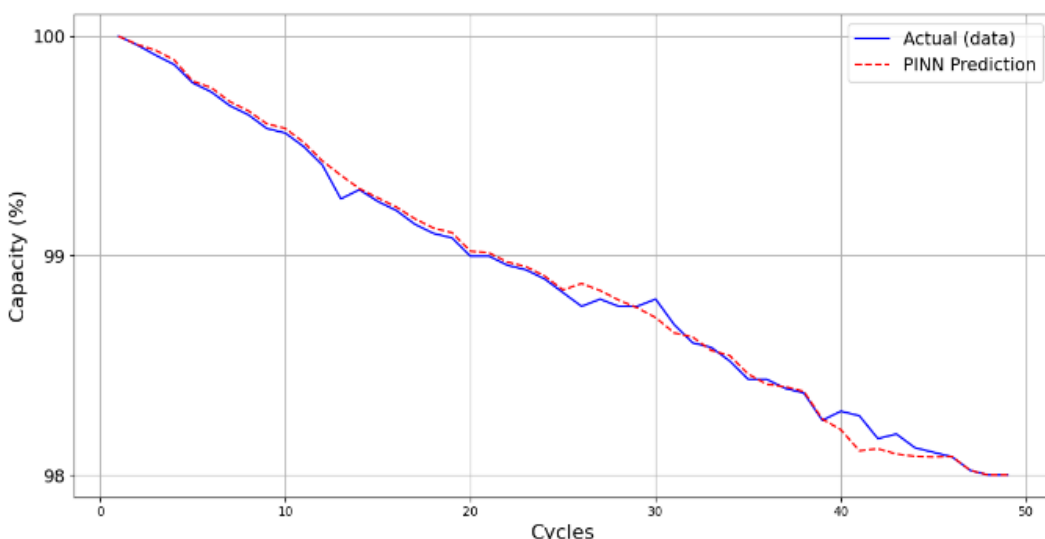


Figure 3. Battery degradation estimation curve compared to the actual value.

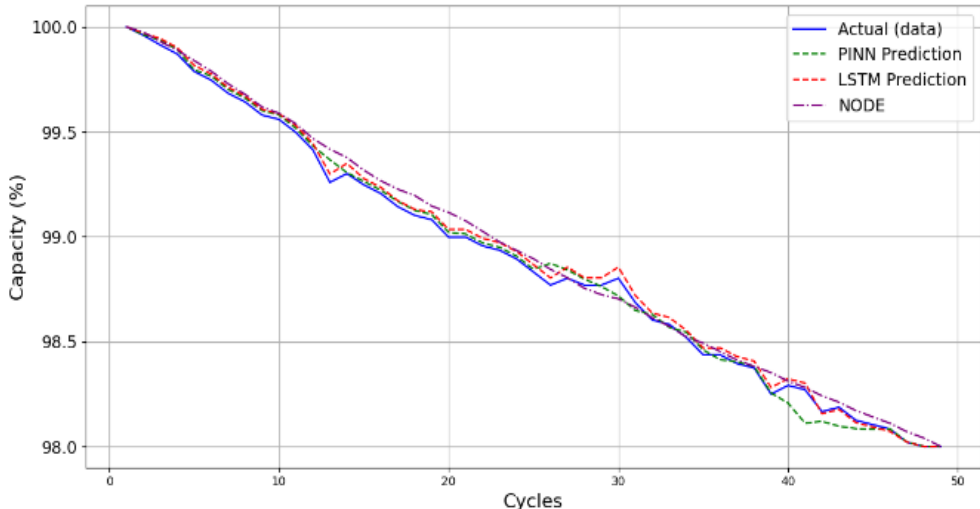


Figure 4. Accuracy comparison between the proposed method, LSTM, and NODE.

All models were trained using the same dataset and input features to ensure a fair comparison. The comparison of battery degradation estimation using these three methods is shown in Figure 4.

Figure 4 illustrates the comparative performance of three different battery degradation prediction models, including LSTM, NODE, and the proposed hybrid model, against actual degradation data over 50 charge-discharge cycles. The figure clearly shows that the LSTM prediction (red dashed line) best matches the actual data trajectory (blue line) in the short term. This is consistent with its numerical performance shown in Table 3, where LSTM achieves the lowest RMSE (0.009) and MAPE (0.68%). However, upon closer inspection, the LSTM model is susceptible to sudden changes in the data, including outliers. For example, in parts of the data where there is a sudden drop in observed degradation, which may be caused by measurement errors or irregular cell performance, the LSTM model tends to follow these unusual changes without any correction or smoothing. This shows that while LSTM can provide accurate predictions at each point, it may not handle noise well and may overfit to noise or unexpected variations in the data.

In contrast, the NODE model exhibits a smoother prediction trajectory that maintains a generally linear trend over the cycles. This is a result of its learning framework, which assumes continuous-time dynamics via neural ordinary differential equations. However, this same structure makes it less responsive to localized changes in the data, especially abrupt variations. As seen in both Figure 4 and Table 3, NODE has the highest RMSE (0.215) and a slightly lower R^2 (0.98), suggesting that while it preserves the overall trend, it systematically deviates from actual

measurements. This limitation may arise from the NODE architecture's implicit bias toward smooth prediction trends, which limits its flexibility in adapting to real-world degradation behavior that is neither completely smooth nor uniform.

The proposed hybrid model, based on PINN, combines recurrent neural structures with physical constraints and offers a balance between the tendency of LSTM models to overfit and the overly smooth behavior seen in NODE-based approaches. When visualized, the predicted curve (green dashed line) aligns well with the actual data, including in areas with small fluctuations or outliers. Rather than directly following these anomalies, the PINN incorporates physical insights into the degradation process, thereby stabilizing and guiding its predictions. This is further supported by quantitative results showing that, while the PINN is slightly less accurate than the LSTM in absolute error, it performs better in terms of generalization. These results strengthen the main argument of this study that integrating physics into learning models can improve robustness and interpretability. Thus, the proposed method contributes to ongoing research by offering a practical alternative to models that rely solely on data, which can compromise long-term reliability, or purely physics-based methods that often struggle to adapt to varying conditions.

Table 3. Accuracy and performance comparison between the proposed method and the previous method

| Metrics | Proposed | LSTM | NODE |
|---------------------|----------|-------|-------|
| RMSE | 0.012 | 0.009 | 0.215 |
| MAPE | 0.97% | 0.68% | 1.27% |
| R-squared (R^2) | 0.99 | 0.99 | 0.98 |

This study also found that the proposed method can produce accurate models with a limited dataset. When sufficient datasets are available, LSTM can produce more accurate models than PINN. However, with a limited dataset, the proposed method maintains its accuracy, whereas LSTM produces models with lower accuracy. The comparison is shown in [Figure 5](#). In this scenario, the LSTM model, which relies entirely on data-driven learning, exhibits significant deviations from the actual battery degradation trend. This is clearly visible in [Figure 5](#), where the LSTM prediction curve shifts significantly below the actual capacity trajectory as the number of cycles increases. This divergence suggests that the LSTM model struggles to generalize when the data is limited or noisy. This may be due to its tendency to overfit or its limited capacity to capture the underlying degradation behavior when the training data is insufficient.

In contrast, the proposed model closely aligns with the actual degradation curve, demonstrating stability and consistency across all cycles. This visual observation is supported by the metrics in [Table 4](#), where the proposed model achieves lower RMSE and MAPE, and a substantially higher R^2 value, than the LSTM model. These results confirm that the proposed model not only captures the overall trend but also maintains predictive accuracy even with reduced data availability.

The robustness of the proposed model stems from its architectural design. Unlike LSTM, which relies solely on learning temporal patterns from data, the PINN framework integrates prior physics knowledge by embedding differential equations describing battery degradation mechanisms directly into the training process.

These physics-based constraints serve as a form of regularization, helping prevent overfitting, guiding the learning process, and enabling the model to capture degradation behavior consistent with physics principles, even when the available data is limited.

These findings strengthen the primary contribution of this study: that incorporating domain-specific physical laws into machine learning models enables the development of data-efficient, generalizable battery degradation models. This is particularly important in real-world applications, where collecting large, high-quality battery datasets can be challenging and expensive. In contrast to previous research that relied solely on data-driven models, this study's results demonstrate a clear move toward a hybrid modeling approach.

Table 4. Accuracy and performance comparison between the proposed method and LSTM within the limited dataset condition

| Metrics | Proposed | LSTM |
|---------------------|----------|-------|
| RMSE | 0.023 | 0.72 |
| MAPE | 1.01% | 6.17% |
| R-squared (R^2) | 0.96 | 0.73 |

Table 5. Computational efficiency comparison between the proposed method and LSTM

| Metrics | Proposed PINN | LSTM |
|----------------------|---------------|--------------|
| Number of Parameters | 261 | 1920 |
| Inference Time | 0.6 ms/sample | 11 ms/sample |
| Memory usage | 49 MB | 566 MB |

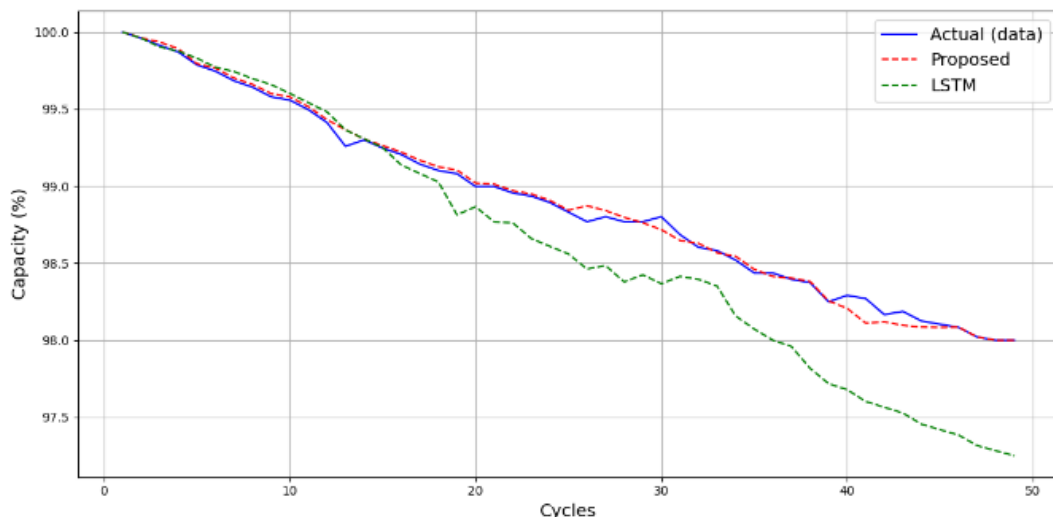


Figure 5. Comparison of the LSTM and PINN models constructed with a limited dataset.

This strategy offers a more balanced solution by combining the interpretability of physics-based models with the predictive power of ML techniques.

In addition to its efficient use of data, the proposed model also demonstrates greater computational efficiency than purely data-driven methods. This is illustrated in [Table 5](#), which presents a comparison of computation parameters, including inference time, memory usage, and number of parameters, between the proposed PINN model and the LSTM model.

The comparison of computational efficiency shows that the proposed PINN method clearly outperforms the LSTM model across model complexity, inference speed, and memory consumption. The PINN model uses a simpler architecture, reducing complexity and resulting in an inference time of 0.6 ms per sample, nearly 18 times faster than the LSTM. It also requires only 49 MB of memory, reflecting a significantly more efficient use of computational resources. This efficiency is primarily attributed to the architecture of the proposed model, which relies on a neural network with only two input features: terminal voltage and current. By limiting the input space to essential physical variables, the model avoids the need for high-dimensional feature extraction or long input sequences, as is common in purely data-driven approaches such as LSTMs. Additionally, by embedding physical knowledge into the learning process, the PINN follows a guided learning path, further reducing the computational burden often associated with modeling long-term dependencies. These findings demonstrate that the physics-informed approach not only achieves strong prediction accuracy with limited data but also significantly lowers computational requirements, making it particularly suitable for real-time applications and deployment in environments with constrained processing and memory resources.

Comparison to Recent Methods

To further assess the performance of the proposed hybrid ANN-Thevenin model and

highlight its contribution to advancing dynamic battery degradation modeling, a comparative analysis is conducted against several existing models from the literature. These models include equivalent circuit models, particularly first- and second-order Thevenin models, as well as various data-driven machine learning techniques, such as RF, XGBoost, GPR, and GRU-based recurrent neural networks (GRU-RNN). Each model was trained and validated on the same dataset, and its performance was evaluated using three standard metrics: RMSE, MAPE, and R^2 . A summary of the results is provided in [Table 6](#).

The comparative analysis in [Table 6](#) highlights the strong performance of the proposed hybrid model. It achieves an RMSE of 0.012, the lowest MAPE of 0.974 %, and a high R^2 of 0.992, matching or even outperforming the best methods from previous studies. These results demonstrate the model's ability not only to capture the overall degradation trend but also to reflect subtle, nonlinear changes in battery condition under dynamic operating conditions. This represents a significant step forward compared to traditional physics-based models, such as the first- and second-order Thevenin models, which yield RMSE values of 1.733 and 1.093, and MAPE values of 8.033% and 6.181%, respectively. The relatively poor performance of these classical approaches highlights their limited capacity to model time-varying degradation, mainly due to simplifying assumptions and the absence of mechanisms to learn from temporal data.

Among the machine learning methods considered, XGBoost demonstrated the strongest performance, with an RMSE of 0.011 and an R^2 value of 0.992, making its accuracy comparable to that of the proposed model. However, XGBoost and other tree-based models, such as RF, rely on static feature extraction and are not inherently designed to capture time-dependent patterns. This issue limits their ability to accurately model battery degradation, as the process is affected by the dynamic factors such as charge-discharge cycles, temperature changes, and variations in state of charge.

Table 6. Performance comparison of the proposed hybrid ANN-Thevenin model with existing methods

| Method | RMSE | MAPE | R-squared (R^2) |
|-------------------------------|--------------|---------------|---------------------|
| The first order Thevenin [10] | 1.733 | 8.033% | 0.715 |
| The second-order Thevenin [7] | 1.093 | 6.181% | 0.765 |
| RF [15] | 0.049 | 1.733% | 0.988 |
| XGBoost [16] | 0.011 | 1.175% | 0.992 |
| GPR [20] | 0.073 | 2.113% | 0.907 |
| GRU-RNN [18] | 0.108 | 1.277% | 0.883 |
| Proposed hybrid method | 0.012 | 0.974% | 0.992 |

Similarly, GPR provides relatively accurate results. However, this method faces scalability challenges when applied to larger datasets and tends to be less effective at capturing rapidly changing degradation patterns.

The GRU-RNN model demonstrates better temporal information handling due to its sequential architecture. However, its overall performance remains lower than that of the proposed hybrid approach. This indicates that although GRU can capture short-term dependencies in the data, it may struggle to generalize to more complex and long-term degradation patterns without the support of physical insights or constraints to guide the learning process.

The effectiveness of the proposed hybrid model lies in integrating the Thevenin equivalent circuit, which provides a physics-based foundation for capturing electrochemical behavior, with an artificial neural network that learns residual nonlinearities and temporal dependencies. This combination allows the model to maintain physical interpretability and strong generalizability, while improving predictive accuracy under dynamic operating conditions. This approach reflects broader developments in the field of battery prognosis, where there is a shift from purely data- or physics-based models towards hybrid frameworks that leverage the complementary strengths of both methodologies.

Thus, instead of simply validating previous results, this study builds on recent advances by demonstrating that a hybrid Thevenin ANN-ECM structure can achieve both high accuracy and robustness in modeling dynamic battery degradation. The proposed method is suitable for practical applications, especially in conditions where data may contain noise and operating conditions change over time.

Limitations and Future Work

While the proposed PINN model demonstrates strong accuracy and robustness in modeling battery degradation, it has been evaluated only on data from the first 50 charge-discharge cycles. This represents only a small portion of the typical lifespan of a lithium-ion battery, which can range from 500 to over 2000 cycles depending on the application. As such, the current study does not fully capture long-term degradation behavior, particularly the nonlinear effects that may emerge after extended cycling.

It is important to note that using early-cycle data in this study assumes that initial degradation patterns reflect the dominant operational behavior in many practical battery applications, especially when early diagnostics are essential for predictive maintenance and system reliability. Early-cycle

performance often provides valuable insight into long-term trends, enabling timely estimation of battery health before significant degradation sets in.

However, the linearity observed during early degradation may not remain consistent throughout the battery's full lifecycle. Therefore, further investigation is needed to validate the model across a broader range of cycles. Future work will focus on extending the training and evaluation of the proposed model using long-term cycling data, covering several hundred to thousands of cycles. This will help assess the model's capability to generalize across different degradation phases and capture complex, nonlinear behavior over time. Additionally, future studies aim to incorporate temperature variations, load profiles, and other real-world operating conditions to enhance the model's applicability in practical battery management systems.

CONCLUSION

This study demonstrates that the proposed PINN model offers an effective and efficient solution for modeling dynamic battery degradation. By integrating physical constraints from the Thevenin equivalent circuit into the learning process, the model achieves a strong balance between predictive accuracy and robustness. When evaluated on 300 charge-discharge cycles of an 18650 LFP cell, the PINN achieved RMSE of 0.012 and MAPE of 0.974 %, outperforming the NODE baseline, which recorded an RMSE of 0.215. While the LSTM model achieved slightly better accuracy with larger datasets, it was more sensitive to noise and showed poor generalization when the data was limited. In contrast, the proposed PINN maintained reliable performance even under reduced training conditions. With a fourfold smaller training set, the PINN retained a low RMSE of 0.023, whereas the LSTM error increased significantly to 0.72. In addition to its predictive performance, the proposed PINN model is also computationally efficient. The final network comprises only 261 parameters, achieves inference speeds of 0.6 ms per sample, and requires only 49 MB of memory. Compared to LSTM, which has higher memory requirements and slower inference, the PINN is significantly better suited for real-time applications, especially in conditions where both data and computational resources are limited. Overall, the results confirm that lightweight neural networks enhanced with physics-based knowledge can offer accurate, robust, and real-time estimation of battery health.

ACKNOWLEDGMENT

This research was supported by the Laboratory of Instrumentation and Control, Department of Electrical Engineering and Information Technology, Universitas Gadjah Mada, Indonesia.

REFERENCES

- [1] Z. Arifin, A. Firmanto, S. Dwirawan, and D. R. Alwani, "Battery Energy Storage System (BESS) as a voltage control at substation based on the defense scheme mechanism," *SINERGI*, vol. 28, pp. 209-218, 2024, doi: 10.22441/sinergi.2024.2.001.
- [2] G. Zhang et al., "Investigation the Degradation Mechanisms of Lithium-Ion Batteries under Low-Temperature High-Rate Cycling," *ACS Appl Energy Mater*, vol. 5, no. 5, pp. 6462-6471, 2022, doi: 10.1021/acsaem.2c00957.
- [3] A. Sarkar, P. Shrotriya, and I. C. Nlebedim, "Parametric analysis of anodic degradation mechanisms for fast charging lithium batteries with graphite anode," *Comput Mater Sci*, vol. 202, 2022, doi: 10.1016/j.commatsci.2021.110979.
- [4] Y. Yang et al., "Modelling and optimal energy management for battery energy storage systems in renewable energy systems: A review," *Renewable and Sustainable Energy Reviews*, vol. 167, 2022, doi: 10.1016/j.rser.2022.112671.
- [5] I. A. Volodin et al., "Beyond steady-state conditions: Chronoamperometric state-of-charge and state-of-health measurements in flow battery electrolytes," *Sens Actuators B Chem*, vol. 403, 2024, doi: 10.1016/j.snb.2023.135101.
- [6] Y. Han, C. Ma, H. Ye, and S. Tang, "Remaining useful life prediction for lithium-ion battery based on the particle filter considering temperature effect," *Journal of Physics: Conference Series*, 2021, doi: 10.1088/1742-6596/2083/2/022100.
- [7] S. Amir et al., "Dynamic Equivalent Circuit Model to Estimate State-of-Health of Lithium-Ion Batteries," *IEEE Access*, vol. 10, pp. 18279-18288, 2022, doi: 10.1109/ACCESS.2022.3148528.
- [8] G. Graber et al., "Modeling of Lithium-Ion Batteries for Electric Transportation: A Comprehensive Review of Electrical Models and Parameter Dependencies," *Energies (Basel)*, vol. 17, no. 22, 2024, doi: 10.3390/en17225629.
- [9] M. Naguib et al., 'Comparative Study between Equivalent Circuit and Recurrent Neural Network Battery Voltage Models', in *SAE Technical Papers*, 2021. doi: 10.4271/2021-01-0759.
- [10] R. O. Nemes et al., "Parameters identification using experimental measurements for equivalent circuit Lithium-Ion cell models," in *2019 11th International Symposium on Advanced Topics in Electrical Engineering, ATEE 2019*, 2019. doi: 10.1109/ATEE.2019.8724878.
- [11] H. Chencheng and L. Jian, "Lithium battery SOC correction technology based on equivalent circuit + UKF filtering algorithm," in *2022 International Conference on Artificial Intelligence and Computer Information Technology, AICIT 2022*, 2022. doi: 10.1109/AICIT55386.2022.9930284.
- [12] Y. Yang, T.-F. Tang, D.-T. Qin, and M.-H. Hu, "PNGV equivalent circuit model and SOC estimation algorithm of lithium batteries for electric vehicle," *Xitong Fangzhen Xuebao / Journal of System Simulation*, vol. 24, no. 4, pp. 938-942, 2012.
- [13] M. Abbas, I. Cho, and J. Kim, "Mathematical Characterization of Experimental Aging Data for Designing Battery Degradation Model," *Journal of Electrical Engineering and Technology*, vol. 18, no. 1, pp. 393-406, 2023, doi: 10.1007/s42835-022-01271-4.
- [14] F. Heinrich, P. Klapper, and M. Pruckner, "A comprehensive study on battery electric modeling approaches based on machine learning," *Energy Informatics*, vol. 4, 2021, doi: 10.1186/s42162-021-00171-7.
- [15] G. Wang, Z. Lyu, and X. Li, "An Optimized Random Forest Regression Model for Li-Ion Battery Prognostics and Health Management," *Batteries*, vol. 9, no. 6, 2023, doi: 10.3390/batteries9060332.
- [16] F. Jiang et al., "An Accurate and Interpretable Lifetime Prediction Method for Batteries using Extreme Gradient Boosting Tree and TreeExplainer," in *2021 IEEE 23rd International Conference on High Performance Computing and Communications, 7th International Conference on Data Science and Systems, 19th International Conference on Smart City and 7th International Conference on Dependability in Sensor, CI*, 2022, pp. 1042-1048. doi: 10.1109/HPCC-DSS-SmartCity-DependSys53884.2021.00164.
- [17] S. Saxena et al., "A convolutional neural network model for battery capacity fade curve prediction using early life data," *J Power Sources*, vol. 542, 2022, doi: 10.1016/j.jpowsour.2022.231736.
- [18] S. Pepe and F. Ciucci, "Long-range battery state-of-health and end-of-life prediction with

neural networks and feature engineering," *Appl. Energy*, vol. 350, 2023, doi: 10.1016/j.apenergy.2023.121761.

[19] M. Safitri, T. B. Adji, and A. I. Cahyadi, "Enhanced early prediction of Li-ion battery degradation using multicycle features and an ensemble deep learning model," *Results in Engineering*, vol. 25, 2025, doi: 10.1016/j.rineng.2025.104235.

[20] R. Zhang, T. Liu, and G. Jin, "Remaining useful life prediction of lithium-ion batteries based on Gaussian process regression with self-constructed kernel," *Xi Tong Gong Cheng Yu Dian Zi Ji Shu/Systems Engineering and Electronics*, vol. 45, no. 8, pp. 2623–2633, 2023, doi: 10.12305/j.issn.1001-506X.2023.08.38.

[21] P. Wang et al., "A comparative study of machine learning based modeling methods for Lithium-ion battery," in *IOP Conference Series: Earth and Environmental Science*, 2020, doi: 10.1088/1755-1315/546/5/052045.

[22] Z. Ren and C. Du, "A review of machine learning state-of-charge and state-of-health estimation algorithms for lithium-ion batteries," *Energy Reports*, vol. 9, pp. 2993–3021, 2023, doi: 10.1016/j.egyr.2023.01.108.

[23] S. Wang et al., "Advanced data-driven techniques in AI for predicting lithium-ion battery remaining useful life: a comprehensive review," *Green Chemical Engineering*, vol. 6, no. 2, pp. 139–153, 2025, doi: 10.1016/j.gce.2024.09.001.

[24] X. Qin et al., "Prognostics of remaining useful life for lithium-ion batteries based on a feature vector selection and relevance vector machine approach," in *2017 IEEE International Conference on Prognostics and Health Management, ICPHM 2017*, 2017, pp. 1–6. doi: 10.1109/ICPHM.2017.7998297.

[25] M. Abbas, I. Cho, and J. Kim, "Mathematical Characterization of Experimental Aging Data for Designing Battery Degradation Model," *Journal of Electrical Engineering and Technology*, vol. 18, no. 1, pp. 393–406, 2023, doi: 10.1007/s42835-022-01271-4.

[26] X. Chen, Y. Yang, J. Song, J. Wang, and G. He, "Hybrid Energy Storage System Optimization with Battery Charging and Swapping Coordination," *IEEE Transactions on Automation Science and Engineering*, vol. 21, no. 3, pp. 4094–4105, 2024, doi: 10.1109/TASE.2023.3292189.

[27] M. D. Ashidqi, A. I. Cahyadi, and A. Ataka, "Capacity Loss Modeling of Li-Ion Battery Using Lightweight Neural Network Considering Equivalent Circuit Model," in *ICT-PEP 2023 - 2023 International Conference on Technology and Policy in Energy and Electric Power: Decarbonizing the Power Sector: Opportunities and Challenges for Renewable Energy Integration*, 2023, pp. 133–138. doi: 10.1109/ICT-PEP60152.2023.10351143.

[28] Y. Fan et al., "A Physics-Informed Integrated Modeling Method for Lithium-ion Batteries," in *Proceedings - 2023 IEEE International Conference on Parallel and Distributed Processing with Applications, Big Data and Cloud Computing, Sustainable Computing and Communications, Social Computing and Networking*, 2023, pp. 868–873. doi: 10.1109/ISPA-BDCloud-SocialCom-SustainCom59178.2023.00146.

[29] J. Brucker, W. G. Bessler, and R. Gasper, "A Grey-box Model with Neural Ordinary Differential Equations for the Slow Voltage Dynamics of Lithium-ion Batteries: Model Development and Training," *J Electrochem Soc*, vol. 170, no. 12, 2023, doi: 10.1149/1945-7111/ad14cd.

[30] J. J. Martinez, M. S. Félix, C. Kulkarni, M. Orchard, and C. Bérenguer, "A novel dynamical model for diagnosis, prognosis and health-aware control of Lithium-ion batteries," in *IFAC-PapersOnLine*, 2024, pp. 658–663. doi: 10.1016/j.ifacol.2024.07.294.

[31] P. Aruna, V. Vasan Prabhu, and V. Krishna Kumar, "Investigation on Physics-Based Models of Lithium-Ion Batteries in Electric Vehicle Applications: A Review," *Recent Advances in Power Electronics and Drives. Lecture Notes in Electrical Engineering*, vol. 973, 2023. doi: 10.1007/978-981-19-7728-2_3.

[32] S. Djelaila, A. A. Tadjeddine, R. I. Bendjillali, and M. S. Bendelhoum, "Beyond a simple filter: transient and steady state analysis of first-order resistor-resistor-capacitor circuits," *Bulletin of Electrical Engineering and Informatics*, vol. 14, no. 6, pp. 4255–4266, 2025, doi: 10.11591/eei.v14i6.10166.

[33] W. Chagra, "Accurate Calculation of the Settling Time of a Linear System Using New Expressions and Iterative Algorithms," *Circuits, Systems, and Signal Processing*, vol. 37, no. 1, pp. 408–431, 2018. doi: 10.1007/s00034-017-0560-3.

[34] I. Izzati, I. K. Sriwana, and S. Martini, "Drug forecasting and supply model design using Artificial Neural Network (ANN) and Continuous Review (r, q) to minimize total supply cost," *SINERGI*, vol. 28, pp. 219–230, 2024. doi: 10.22441/sinergi.2024.2.002.